Porous Molecules

DOI: 10.1002/ange.201006030

On–Off Porosity Switching in a Molecular Organic Solid**

*James T. A. Jones, Daniel Holden, Tamoghna Mitra, Tom Hasell, Dave J. Adams, Kim E. Jelfs, Abbie Trewin, David J. Willock, Graeme M. Day, John Bacsa, Alexander Steiner, and Andrew I. Cooper**

The selective uptake of guests in molecular-sized channels underpins function in biological membranes[1,2] and in materials for molecular separations.[3,4] Synthetic porous networks can respond structurally towards guest sorption[5–8] suggesting applications, for example, as enzyme mimics.[8] We report here an organic cage molecule[9,10] where the porosity can be switched on and off in response to a chemical stimulus. The cage can exist in three different polymorphic forms which are nonporous, selectively porous to hydrogen gas, and non-selectively porous. The first two forms can be interconverted reversibly in the solid state by exposure to organic trigger molecules which encode specifically for these polymorphs. This "on–off" porosity transformation is reversible and involves conformational changes in the organic cage as well as repositioning of the cages in the soft crystal lattice.

Synthetic molecular networks can respond structurally to guest sorption[5–7] and may therefore exhibit behavior that is more complex than their static 3-dimensional molecular structures implies. Molecular crystals such as calixarenes[11,12] and clathrates[13,14] can also adsorb guests through cooperative diffusion mechanisms. By contrast, classical, permanent pore structures in molecular crystals are comparatively rare.[15–19] Unlike porous networks,[20–24] porous molecular crystals have extended structures that are not defined by strong directional covalent or coordination bonding. This opens the possibility of dramatic guest-induced changes which may involve both reorientation and positional translation of the discrete molecular subunits.

We show here that an organic cage molecule, **1**, can interconvert in the solid state between three polymorphs (nonporous, **1α**; selectively porous, **1β**; and non-selectively porous, **1γ**; Figure 1) in response to specific chemical triggers.

The porosity in two of these polymorphs, **1α** and **1β**, can be interconverted reversibly in the solid state whereas the non-selectively porous form, **1γ**, shows only limited reversibility. On–off porosity switching might be useful in the future for controlling permeation or in capturing particular guests in a "molecular mousetrap".

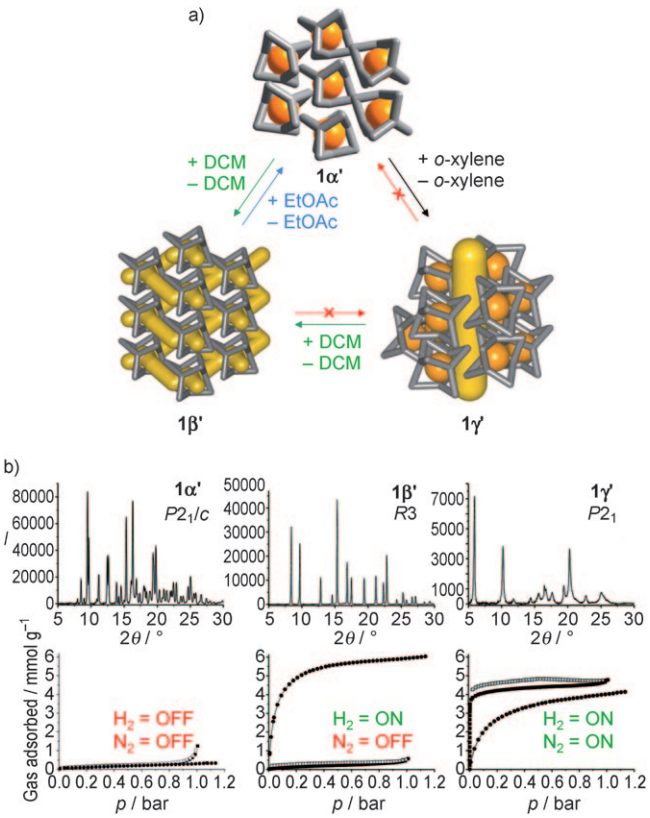

Figure 1. Solid-state "on–off" porosity switching. a) Exposure of the nonporous phase, **1α′**, to different trigger molecules (dichloromethane (DCM) and *ortho*-xylene) directs the structure into one of two porous forms, **1β′** and **1γ′**. The packing motifs are shown with isolated void volume and interconnected pore channels illustrated in orange and yellow, respectively. The **1α′** and **1β′** packings are derived from single crystal structures; the $P2_1$ **1γ′** structure is a model based on Le Bail fitting (Supporting Information, Figure S8). As illustrated in this scheme, the **1α′**⇔**1β′** switch is reversible while the **1α′**/**1γ′** and **1β′**/**1γ′** transitions are not. b) Powder XRD patterns for the bulk materials after guest removal. Corresponding nitrogen and hydrogen gas sorption data at 77 K are also shown (squares and circles, respectively). **1γ′** is porous to both N_2 and H_2 while **1β′** is selectively porous to H_2 only.

[*] Dr. J. T. A. Jones, D. Holden, Dr. T. Mitra, Dr. T. Hasell, Dr. D. J. Adams, Dr. K. E. Jelfs, Dr. A. Trewin, Dr. J. Bacsa, Dr. A. Steiner, Prof. A. I. Cooper
Department of Chemistry and Centre for Materials Discovery
University of Liverpool, Crown Street, Liverpool (UK)
Fax: (+44) 151-794-2304
E-mail: aicooper@liv.ac.uk
Dr. D. J. Willock
Cardiff Catalysis Institute, School of Chemistry
Cardiff University, Main Building, Cardiff, CF10 3AT (UK)
Dr. G. M. Day
Department of Chemistry, University of Cambridge
Lensfield Road, Cambridge, CB2 1EW (UK)

[**] We thank the Engineering and Physical Sciences Research Council (EPSRC) for funding (EPSRC/C511794 & EP/H000925/1). A.C. is a Royal Society Wolfson Research Merit Award holder. A.T. and G.D. are Royal Society University Research Fellows.

Supporting information for this article is available on the WWW under http://dx.doi.org/10.1002/anie.201006030.

The organic cage, **1**, was synthesized using ethyl acetate (EtOAc) as the solvent as described previously.[9] This tetrahedral molecule is around 1 nm in size and consists of four arene faces connected by six aliphatic linkers (Scheme 1). Each cage comprises four nearly triangular windows. The material is isolated as a solvate, **1α**·2.5 EtOAc, which can be desolvated by heating (step (1) in Figure 2).

This causes a single-crystal-to-single-crystal (SC-SC) transformation[25] leading to a structure with disconnected cage voids, **1α′**, which is nonporous to gases such as N_2 and H_2 at 77 K.[9] This process is reversible and **1α′** can be resolvated by exposure to EtOAc vapour (step (2); Figure 2). To demonstrate the solid-state switching concept, crystals of **1α′** were exposed to dichloromethane (DCM) vapor (step (3); Figure 2, see Supporting Information) followed by complete desolvation under dynamic vacuum at 100 °C (step (4); Figure 2). This triggers a solid-state transformation to a new polymorph, **1β′**. The switching procedure is reversible since exposure of **1β′** to EtOAc vapor regenerates the **1α** polymorph (step (6); Figure 2). X-ray structure analysis of single crystals grown from a solution of **1** in DCM revealed a solvate, **1β**·2.5 DCM. Surprisingly, the **1β**·2.5 DCM structure contains two conformers of **1**: the familiar tetrahedral cage molecule[9,10] $\mathbf{1}^{T}$ and also a non-tetrahedral conformer with threefold symmetry, $\mathbf{1}^{C3}$ (Figures S2, S3). The two conformers $\mathbf{1}^{T}$ and $\mathbf{1}^{C3}$ exist in a 1:1 ratio in the **1β**·2.5 DCM structure and are stacked in an alternating fashion through window-to-arene interactions along the crystallographic three-fold axis. Neighboring stacks are shifted with respect to each other by 1/3 in *z* forming a helical channel (in yellow, Figure 2a) running around the 3_1 screw axes. The channel is occupied by DCM molecules. The **1β′** phase therefore contains an interconnected channel structure, unlike the disconnected cage voids observed in **1α′**.

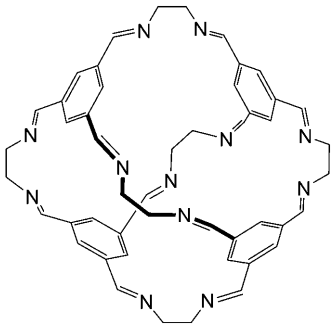

Scheme 1. Tetrahedral [4+6] organic cage molecule **1**.

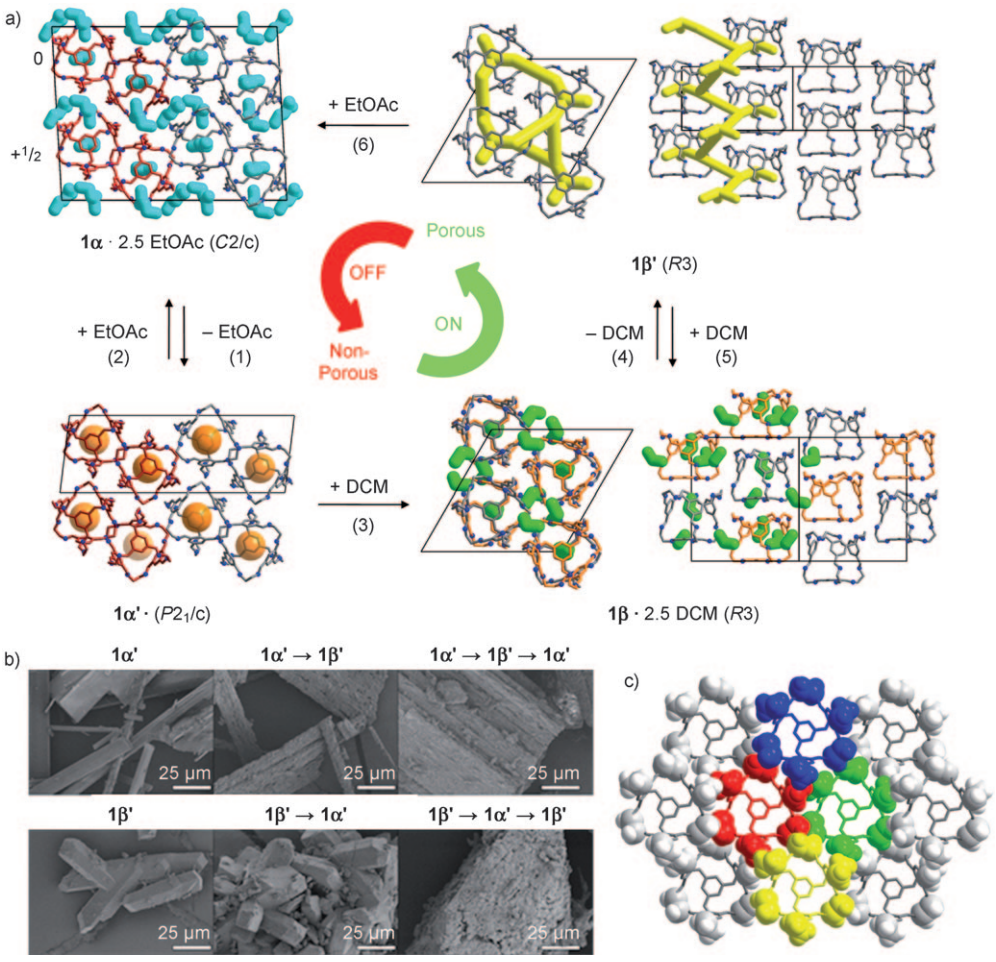

Figure 2. Conformational flexibility allows reversible solid-state porosity switching in a "soft" molecular organic crystal. a) Reversible "on–off" switching mechanism illustrated by single-crystal structures for guest-occupied and guest-free polymorphs of **1** (counter-clockwise from top left): **1α**·2.5 EtOAc (EtOAc shown in blue), **1α′**, **1β**·2.5 DCM (DCM shown in green) and **1β′**. The red and gray molecules in **1α**·2.5 EtOAc and **1α′** indicate *R* and *S* cages, respectively. The orange cages in **1β**·2.5 DCM represent non-tetrahedral $\mathbf{1}^{C3}$ conformers, the tetrahedral $\mathbf{1}^{T}$ cages are shown in gray. Crystallographic space groups are given in parentheses. **1β′** is shown arbitrarily as the *S* enantiomer; the overall system is a chiral conglomerate. b) Electron micrographs of desolvated crystals of **1** obtained in the solid-state interconversion between **1α′** and **1β′** polymorphs by exposure to organic vapor. The top and bottom rows of images represent "off–on–off" and "on–off–on" sequences, respectively. The average crystallite size is reduced through successive switching transformations but PXRD (Figure 3) confirms that long-range crystallographic order is retained. c) Scheme illustrating how the packing of ethane vertex groups, shown here in a space-filling representation, locks **1β′** into an open, porous structure and prevents collapse to the denser **1α′** form.

When heated to 60 °C in situ in the diffractometer, single crystals of **1β**·2.5 DCM grown from DCM solution lose most of their organic guests while retaining macroscopic integrity. The X-ray structure confirmed the preservation of the 3D channel network and revealed the absence of guests in the helical channels while residual electron density, equivalent to 0.66 molecules of DCM, was found in the cage interior. Bulk, powdered **1β**·2.5 DCM material was also completely desolvated by heating under dynamic vacuum. Powder X-ray diffraction (PXRD; Figure S4, S5) for this fully desolvated **1β′** sample suggested the same structure as the partially desolvated single crystal. This shows that it is possible to retain the molecular order in the crystal upon complete desolvation but not the single crystal morphology. The molecular packing in **1β′** resembles solvated **1β** but consists purely of $\mathbf{1}^{\mathbf{T}}$ tetrahedral cages: that is, the $\mathbf{1}^{\mathbf{C3}}$ conformer converts in the solid state into $\mathbf{1}^{\mathbf{T}}$ during the **1β**→**1β′** transformation (step (4); Figure 2a). This isomerization requires the six imino groups which are part of the window–arene interaction to rotate 180° around the $C_{(imino)}$–$C_{(arene)}$ bonds. The result is a homochiral crystal containing cages $\mathbf{1}^{\mathbf{T}}$ of one enantiomer only. It should be noted that the equivalent rotation of the other six imino groups in $\mathbf{1}^{\mathbf{C3}}$ would generate a tetrahedral cage $\mathbf{1}^{\mathbf{T}}$ of the opposite enantiomer. The morphology of larger crystals of **1β** produced by recrystallization suggests a chiral conglomerate (Figure S6). The structure for a single crystal of **1β** provides a snapshot for understanding the solid-state, vapor-induced **1α′**→**1β′** switching mechanism in the bulk powder. The presence of the $\mathbf{1}^{\mathbf{C3}}$ conformer shows that intramolecular conformational changes play a key role in addition to translational reorganization of the molecular subunits in the crystal lattice. The ability to invert chirality in $\mathbf{1}^{\mathbf{T}}$ through conformers such as $\mathbf{1}^{\mathbf{C3}}$ rationalizes the solid-state interconversion between racemic (**1α′**, space group $P2_1/c$) and chiral domains (**1β′**, space group $R3$) in the absence of substantial mass transport between crystallites. Cage **1** behaves therefore as a "soft"[7] porous crystal in the interconversion of these polymorphs. The scope for conformational switching in **1** is supported by variable temperature ^{1}H NMR studies which show that its configuration interconverts rapidly in solution, even at temperatures as low as 230 K (Figure S7). DFT calculations show that the discrete $\mathbf{1}^{\mathbf{T}}$ conformer lies 13 kJ mol^{-1} lower in energy than $\mathbf{1}^{\mathbf{C3}}$, indicating that the presence of $\mathbf{1}^{\mathbf{C3}}$ is compensated by net-favorable packing interactions in the **1β**·2.5 DCM lattice.

Both of the desolvation processes (**1α**→**1α′**, step (1), and **1β**→**1β′**, step (4) in Figure 2) give rise to relatively subtle structural changes. In **1α** and **1α′**, cage $\mathbf{1}^{\mathbf{T}}$ is assembled in layers parallel to the (0 1 0) plane. These layers move closer together upon removal of intercalated EtOAc molecules, as manifested in a 12% reduction in volume, V/Z, and a 5 Å lateral shift of the layers parallel to each other. This puts strain on the crystal which becomes highly mosaic in the process. By contrast, **1β**→**1β′** constitutes a smooth transition, facilitated by the conformational flexibility of **1**, which reduces the volume by only 3%.

The two vapor-triggered phase switching transformations, **1α′**→**1β**, step (3), and **1β′**→**1α**, step (6), are accompanied by more substantial reorientation of cages in the crystal lattice. The resulting products are highly crystalline and phase-pure, but SEM images show that macroscopic crystal integrity deteriorates in the process (Figure 2b; Figures S19–21). The guest-triggered **1α′**→**1β** transformation is presumably aided by a cooperative dynamic process[12,26] where local free volume is created to allow DCM to penetrate the formally nonporous **1α′** phase. Calculations based on an empirical repulsion–dispersion model and multipolar electrostatics show that the energies of **1β′** and **1α′** are almost identical ($E_{latt} = -173.2$ and -173.5 kJ mol^{-1}, respectively), indicating that switching does not have to overcome a substantial inherent stability difference. Likewise, there is no experimental evidence for one desolvated polymorph transforming into another over time, nor does heating or energy-intensive ball milling appear to induce any interconversion between the **1α′** and **1β′** polymorphs. These calculations and observations suggest a balanced system which facilitates the reversible, solvent-triggered switch. It is notable that the **1β′** crystals retain a permanent pore structure and do not revert upon guest removal to a more compact arrangement, such as **1α′**, through chiral interconversion of 50% of the cages. Close inspection of the crystal structure for **1β′** shows that the ethane vertex groups of neighbouring stacks are packed to lock the structure into an open, self-supporting arrangement (Figure 2c). When crystals of **1β′** are exposed to EtOAc vapor, the trigger molecule is incompatible with the helical 3D pore structure. Hence, the material transforms to the intercalated **1α** phase, again through a process of conformational interconversion to convert chiral domains into racemic domains (Figure 2a; step (6)).

Solid-state switching between nonporous **1α′** and selectively porous **1β′** can be carried out over successive cycles without loss of crystallinity by exposing the solid to the EtOAc trigger (to form **1α**) or the DCM trigger (to form **1β**) followed by guest removal. Figure 3 shows this process for two cycles and illustrates that long-range crystallographic order is retained both for the "on–off–on" and for "off–on–off" sequences (see Figure S13 for the latter). We suggest that the reversibility is facilitated by the high-symmetry tetrahedral $\mathbf{1}^{\mathbf{T}}$ structure which both reduces entropy changes and allows a variety of cage–cage interactions. The low-energy interconversion between cage conformers facilitates smooth rearrangements in the soft molecular crystal. The uniquely dynamic pore structure is therefore a function of both intermolecular and intramolecular rearrangements in crystalline **1**.

The **1β′** polymorph exhibits highly selective gas uptake. It is nonporous to both N_2 and argon at 77 K but adsorbs significant quantities of H_2 (Figure 1b).[27,28] This selectivity can be rationalized by the single-crystal structure. A solvent-accessible surface[28] calculated using a probe radius of 0.142 nm (the kinetic radius for H_2) shows the pore channels to be interconnected (Figure 4a). By contrast, a surface produced using a probe radius of 0.182 nm (the kinetic radius for N_2) shows disconnected cavities (Figure 4b). In principle, **1β′** might nonetheless be porous to N_2 as a result of cooperative diffusion mechanisms[12] but this is not observed in molecular dynamics (MD) simulations, even at 395 K (Figure 4a,b). MD simulations of H_2 diffusion in **1β′** support

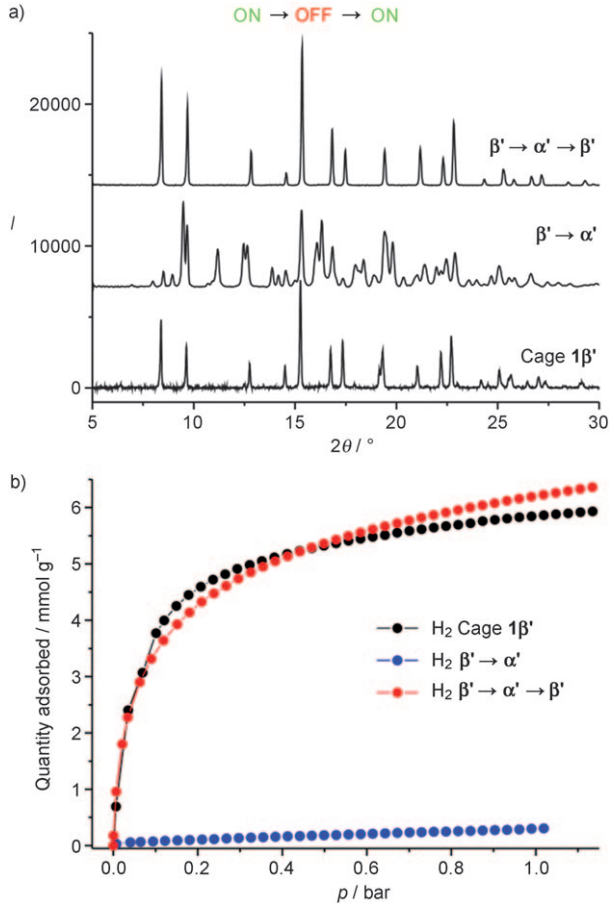

Figure 3. Solid-state porosity switching allows reversible gating of H_2 sorption. a) PXRD patterns for the desolvated structures showing **1α′⇔1β′** porosity switching. Although the crystal morphology is affected strongly by switching (Figure 2b), the long-range molecular order is retained over the "on–off–on" sequence. b) H_2 adsorption isotherms measured at 77 K for the desolvated phases illustrating reversible gating of gas sorption. The equivalent "off–on–off" sequence is also reversible, see Figure S13.

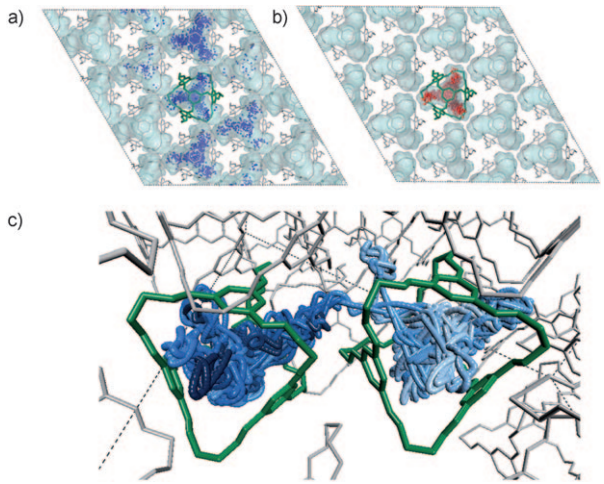

Figure 4. Molecular dynamics simulations rationalizing H_2 selectivity for **1β′**. a,b) Molecular dynamics (MD) simulations with an NPT ensemble at 395 K for H_2 (a) and N_2 (b) in **1β′** showing overlaid solvent-accessible surface (pale blue) constructed using probe radii of 1.42 Å and 1.82 Å, respectively (500 ps, timestep 5 fs, sampling every 1000 steps). Hydrogen (blue) diffuses between cages in this simulation but N_2 (red) does not. c) Detail of MD simulation showing diffusion pathway for H_2 between two cages highlighted in green (125 ps, timestep 5 fs, sampling every step) suggesting a "hopping" mechanism. The trajectory of the H_2 molecule is shown in blue (light blue = start of simulation, dark blue = end of simulation).

the observed selectivity, suggesting a hopping mechanism where the H_2 residence time in channels between the cages is relatively short (Figure 4c). This is consistent with the narrow pore neck between the cages, which is evident in the marginally interconnected surface shown in Figure 4a.

Revealingly, additional MD simulations which treat the cages as static entities did not reveal H_2 diffusion between cages, suggesting that cooperative diffusion mechanisms might operate in **1β′** even for a sorbate as small as dihydrogen. The **1β′** polymorph adsorbs 5.9 mmol g^{-1} H_2 (1.18 wt.%) at 1.2 bar/77 K.

In its current form, the "on–off" pore switching mechanism involves solvation followed by desolvation. This might be inconvenient for many applications, however the adaptive pore structure in **1** does suggest potential uses in selective guest trapping. This is illustrated by the differential response of **1β′** to the two trigger molecules, DCM and EtOAc. Both triggers produce solvates when their vapors are contacted with **1β′**. However, DCM induces relatively minor structural changes involving conformational switching of $\mathbf{1}^{T}$ to $\mathbf{1}^{C3}$ but hardly any molecular translation in the crystal lattice (step (5); Figure 2a). By contrast, EtOAc triggers a more profound switch to the nonporous **1α**·2.5 EtOAc phase, step (6), and the trapped EtOAc guest is only removed at temperatures substantially above its boiling point (> 110 °C; Figure S15). As such, EtOAc triggers a "molecular mousetrap" whereas DCM does not. These results suggest that more sensitive traps could be designed and that similar materials might capture more weakly interacting guests such as CO_2 or perhaps even H_2. Extension of the strategy to larger cages and guests should also be possible, drawing on the diverse cage-forming chemistry that has been developed.[30]

Experimental Section

Cage **1** was synthesized as described previously.[9] The solid-state polymorph conversions were performed using a "vial in vial" technique whereby the desolvated cage **1** (80 mg) was placed in an open vial which was then placed into a larger vial containing the organic trigger molecule (ethylacetate, *o*-xylene or DCM). The large vial was then sealed and left at room temperature for 3 d. Care was taken never to allow the liquid solvent to come into direct contact with the dry powdered sample. Molecular dynamics calculations were carried out using a customized atomic force field, see Supporting Information.

Received: September 26, 2010
Published online: November 12, 2010

Keywords: conformers · cooperative diffusion · microporous materials · molecular cages

[1] K. Murata, K. Mitsuoka, T. Hirai, T. Walz, P. Agre, J. B. Heymann, A. Engel, Y. Fujiyoshi, *Nature* **2000**, *407*, 599.
[2] R. MacKinnon, *Angew. Chem.* **2004**, *116*, 4363; *Angew. Chem. Int. Ed.* **2004**, *43*, 4265.
[3] T. C. Merkel, B. D. Freeman, R. J. Spontak, Z. He, I. Pinnau, P. Meakin, A. J. Hill, *Science* **2002**, *296*, 519.
[4] J. R. Li, R. J. Kuppler, H. C. Zhou, *Chem. Soc. Rev.* **2009**, *38*, 1477.
[5] D. Bradshaw, J. E. Warren, M. J. Rosseinsky, *Science* **2007**, *315*, 977.
[6] C. Serre, C. Mellot-Draznieks, S. Surble, N. Audebrand, Y. Filinchuk, G. Férey, *Science* **2007**, *315*, 1828.
[7] S. Horike, S. Shimomura, S. Kitagawa, *Nat. Chem.* **2009**, *1*, 695.
[8] J. Rabone, Y. F. Yue, S. Y. Chong, K. C. Stylianou, J. Bacsa, D. Bradshaw, G. R. Darling, N. G. Berry, Y. Z. Khimyak, A. Y. Ganin, P. Wiper, J. B. Claridge, M. J. Rosseinsky, *Science* **2010**, *329*, 1053.
[9] T. Tozawa, J. T. A. Jones, S. I. Swamy, S. Jiang, D. J. Adams, S. Shakespeare, R. Clowes, D. Bradshaw, T. Hasell, S. Y. Chong, C. Tang, S. Thompson, J. Parker, A. Trewin, J. Bacsa, A. M. Z. Slawin, A. Steiner, A. I. Cooper, *Nat. Mater.* **2009**, *8*, 973.
[10] T. Hasell, X. F. Wu, J. T. A. Jones, J. Bacsa, A. Steiner, T. Mitra, A. Trewin, D. J. Adams, A. I. Cooper, *Nat. Chem.* **2010**, *2*, 750.
[11] J. L. Atwood, L. J. Barbour, A. Jerga, *Science* **2002**, *296*, 2367.
[12] J. L. Atwood, L. J. Barbour, A. Jerga, B. L. Schottel, *Science* **2002**, *298*, 1000.
[13] S. A. Allison, R. M. Barrer, *J. Chem. Soc. A* **1969**, 1717.
[14] J. L. Flippen, J. Karle, I. L. Karle, *J. Am. Chem. Soc.* **1970**, *92*, 3749.
[15] C. G. Bezzu, M. Helliwell, J. E. Warren, D. R. Allan, N. B. McKeown, *Science* **2010**, *327*, 1627.
[16] K. J. Msayib, D. Book, P. M. Budd, N. Chaukura, K. D. M. Harris, M. Helliwell, S. Tedds, A. Walton, J. E. Warren, M. Xu, N. B. McKeown, *Angew. Chem.* **2009**, *121*, 3323; *Angew. Chem. Int. Ed.* **2009**, *48*, 3273.
[17] A. C. Sudik, A. R. Millward, N. W. Ockwig, A. P. Côté, J. Kim, O. M. Yaghi, *J. Am. Chem. Soc.* **2005**, *127*, 7110.
[18] J. R. Holst, A. Trewin, A. I. Cooper, *Nat. Chem.* **2010**, *2*, 915.
[19] L. J. Barbour, *Chem. Commun.* **2006**, 1163.
[20] O. M. Yaghi, M. O'Keeffe, N. W. Ockwig, H. K. Chae, M. Eddaoudi, J. Kim, *Nature* **2003**, *423*, 705.
[21] S. Kitagawa, R. Kitaura, S. Noro, *Angew. Chem.* **2004**, *116*, 2388; *Angew. Chem. Int. Ed.* **2004**, *43*, 2334.
[22] G. Férey, C. Mellot-Draznieks, C. Serre, F. Millange, J. Dutour, S. Surble, I. Margiolaki, *Science* **2005**, *309*, 2040.
[23] A. P. Côté, A. I. Benin, N. W. Ockwig, M. O'Keeffe, A. J. Matzger, O. M. Yaghi, *Science* **2005**, *310*, 1166.
[24] J.-X. Jiang, F. Su, A. Trewin, C. D. Wood, N. L. Campbell, H. Niu, C. Dickinson, A. Y. Ganin, M. J. Rosseinsky, Y. Z. Khimyak, A. I. Cooper, *Angew. Chem.* **2007**, *119*, 8728; *Angew. Chem. Int. Ed.* **2007**, *46*, 8574.
[25] C. L. Chen, A. M. Goforth, M. D. Smith, C. Y. Su, H. C. zur Loye, *Angew. Chem.* **2005**, *117*, 6831; *Angew. Chem. Int. Ed.* **2005**, *44*, 6673.
[26] D. Das, E. Engel, L. J. Barbour, *Chem. Commun.* **2010**, *46*, 1676.
[27] B. L. Chen, S. Q. Ma, F. Zapata, F. R. Fronczek, E. B. Lobkovsky, H. C. Zhou, *Inorg. Chem.* **2007**, *46*, 1233.
[28] Y. E. Cheon, M. P. Suh, *Chem. Eur. J.* **2008**, *14*, 3961.
[29] T. Düren, F. Millange, G. Férey, K. S. Walton, R. Q. Snurr, *J. Phys. Chem. C* **2007**, *111*, 15350.
[30] M. Masterlerz, *Angew. Chem.* **2010**, *122*, 5164; *Angew. Chem. Int. Ed.* **2010**, *49*, 5042.